

## Measurement of the Charge-Density-Wave Correlation Length in NbSe<sub>3</sub> by High-Resolution X-Ray Scattering

E. Sweetland, C-Y. Tsai, B. A. Wintner, and J. D. Brock

*School of Applied and Engineering Physics and Materials Science Center, Cornell University, Ithaca, New York 14853*

R. E. Thorne

*Laboratory of Atomic and Solid State Physics and Materials Science Center, Cornell University, Ithaca, New York 14853*

(Received 9 August 1990)

We have measured the correlation length of the  $q_1$  charge-density wave in NbSe<sub>3</sub> using high-resolution x-ray scattering. For a heavily Ta-doped crystal having a residual-resistivity ratio  $r_R$  of 10, the  $T=77$  K correlation lengths parallel and transverse to the quasi-one-dimensional  $\mathbf{b}^*$  direction are  $l_{b^*} \approx 0.9 \mu\text{m}$  and  $l_{a^*} \approx 0.1 \mu\text{m}$ , respectively. For an undoped crystal ( $r_R \approx 300$ ), we obtain lower bounds  $l_{b^*} \approx 2.5 \mu\text{m}$  and  $l_{a^*} \approx 1.9 \mu\text{m}$ , the latter value being comparable to the thickness of typical crystals. These results are in excellent agreement with a recent weak-impurity-pinning analysis of finite-size effects observed in transport properties.

PACS numbers: 72.15.Nj

The character of charge-density-wave (CDW) pinning in quasi-one-dimensional conductors such as NbSe<sub>3</sub> has been the subject of controversy for nearly a decade. Two types of pinning are distinguished. In weak pinning, the CDW phase is pinned by impurity fluctuations, and the length scale on which the phase varies is much greater than the average impurity spacing.<sup>1</sup> In strong pinning, the CDW phase is pinned at each impurity site.<sup>1,2</sup> Most studies of pinning have focused on the dependence of the threshold electric field necessary to induce CDW motion,  $E_T$ , on the impurity concentration  $n_i$ . Early measurements<sup>3</sup> on Ta-doped NbSe<sub>3</sub> were consistent with weak pinning, whereas subsequent measurements have been consistent with strong pinning,<sup>4</sup> or have yielded ambiguous results.<sup>5</sup>

Recently, McCarten *et al.*<sup>6</sup> showed that the dependence of  $E_T$  on crystal cross-sectional dimensions reported by Borodin *et al.*<sup>7</sup> and by Yetman and Gill<sup>8</sup> must be accounted for when evaluating the effects of impurities. In large NbSe<sub>3</sub> crystals,  $E_T$  varies with Ta concentration  $n_i$  as  $E_T \propto n_i^2$ . In small crystals,  $E_T \propto n_i/t$ , where  $t$  is the crystal thickness. These results are consistent with weak CDW pinning in three and two dimensions, respectively,<sup>9</sup> and suggest that a crossover from 3D to 2D pinning occurs when the transverse CDW phase-phase correlation length  $l_{a^*}$  is comparable to the crystal thickness. For the  $q_1$  CDW in undoped NbSe<sub>3</sub> at  $T=77$  K, McCarten *et al.* deduced transverse and longitudinal correlation lengths on the order of 1 and 10  $\mu\text{m}$ , respectively. The correlation lengths along these two directions deduced from other measurements<sup>10</sup> are factors of 50 and 5 smaller. Consequently, McCarten *et al.*'s interpretation has stimulated considerable debate.<sup>10,11</sup>

Here we report direct measurements of the  $q_1$  CDW correlation lengths in pure and Ta-doped NbSe<sub>3</sub> using high-resolution synchrotron x-ray scattering. In pure crystals, the transverse correlation length  $l_{a^*}$  is on the or-

der of 1  $\mu\text{m}$ . In doped crystals, the transverse correlation length decreases approximately linearly with increasing impurity concentration, and the ratio of the longitudinal to transverse correlation length is approximately 10:1. These results have broad implications for the study of sliding-CDW systems.

NbSe<sub>3</sub> has a monoclinic unit cell with lattice parameters  $a=10.009 \text{ \AA}$ ,  $b=3.480 \text{ \AA}$ ,  $c=15.629 \text{ \AA}$ , and  $\beta=109.47^\circ$ .<sup>12</sup> Single crystals prepared by vapor transport have the form of thin, ribbonlike whiskers. Crystal lengths can be several centimeters, thicknesses vary from 0.1 to 10  $\mu\text{m}$ , and widths are typically 10 times larger than the thickness. The ribbon axis corresponds to the highly conducting  $\mathbf{b}^*$  direction. The thickness  $t$  is measured along the  $\mathbf{a}^*$  direction. Independent CDWs form at  $T_{P_1}=145$  K and  $T_{P_2}=59$  K with wave vectors  $\mathbf{q}_1=(0, 0.241, 0)$  and  $\mathbf{q}_2=(0.5, 0.260, 0.5)$ . When an electric field greater than a threshold field  $E_T$  is applied, CDW motion occurs along  $\mathbf{b}^*$ .

In kinematic scattering theory, the intensity of scattered x rays at a CDW satellite peak is given by

$$I(\mathbf{Q}) \propto \int d\mathbf{r} e^{i\mathbf{Q} \cdot \mathbf{r}} \langle \Psi(\mathbf{0}) \Psi^*(\mathbf{r}) \rangle,$$

where  $\mathbf{Q}$  is the scattering vector and  $\Psi(\mathbf{r}) = \Delta(\mathbf{r}) e^{i\phi(\mathbf{r})}$  is the complex CDW order parameter. Therefore, the width of the superlattice diffraction peak is inversely proportional to the equal-time CDW correlation length. At temperatures well below the Peierls transition, amplitude fluctuations can be neglected, and the CDW correlation length is determined by the phase-phase correlation length. Thus, x-ray-scattering measurements directly probe the quantity of interest in a model-independent manner.

The x-ray-scattering measurements were performed on the A-2 beam line at the Cornell High Energy Synchrotron Source (CHESS). Using radiation from the six-

pole wiggler, a double-bounce monochromator consisting of two perfect Si(311) crystals selected an x-ray wavelength of 1.5 Å. Sample and detector motions were provided by a six-circle diffractometer. The scattered x rays were analyzed either by two sets of tantalum slits or by a Si(311) crystal analyzer and then detected by a NaI(Tl) scintillation counter. NbSe<sub>3</sub> single crystals were attached using silver and graphite paint to the tip of a pointed copper post, and then mounted inside a closed-cycle helium refrigerator. Because its vibrations broadened the diffraction-peak widths to several hundredths of a degree, the refrigerator was turned off during the measurements. Temperature drift during a given scan was typically between 0.2 and 1 K. To facilitate comparisons with the electrical measurements of Ref. 6, the scattering measurements were performed on the q<sub>1</sub> CDW at T ≈ 77 K. This temperature also corresponds to that of the refrigerator's radiation shield, and thus minimized both temperature drift and gradients across the sample.

Previous high-resolution x-ray measurements by Fleming *et al.*<sup>13</sup> and by Moudden *et al.*<sup>14</sup> on undoped NbSe<sub>3</sub> at T ≪ T<sub>P</sub> have yielded a lower bound for the q<sub>1</sub> CDW correlation length along b\* of l<sub>b\*</sub> ≈ 4000 Å. Measurement of the transverse correlation length l<sub>a\*</sub> has been prevented by large mosaic widths, although Moudden *et al.*<sup>14</sup> obtained an anisotropy ξ<sub>b\*</sub>/ξ<sub>a\*</sub> ≈ 3.5 for the CDW fluctuations above T<sub>P</sub>. Our measurements differ from previous experiments in three ways. First, we have used high-quality NbSe<sub>3</sub> crystals having very small mosaic widths, allowing direct measurement of l<sub>a\*</sub>. Second, we have improved our resolution by using Si(311) mono-

chromator and analyzer crystals, which make scattering near the (1̄,2,0) Bragg peak and the (1̄,2-q<sub>1</sub>,0) CDW peak nearly nondispersive. Third, in addition to high-purity undoped NbSe<sub>3</sub> crystals, we have studied crystals heavily doped with Ta to ensure that the correlation lengths are resolved. The residual-resistivity ratios r<sub>R</sub> = R(300 K)/R(4.2 K) and threshold electric fields E<sub>T</sub> range from r<sub>R</sub> ≈ 300 and E<sub>T</sub>(77 K) ≈ 0.05 V/cm for the undoped crystals to r<sub>R</sub> ≈ 10 and E<sub>T</sub>(77 K) ≈ 10 V/cm for the most heavily doped crystals.<sup>15</sup>

Figure 1 compares mosaic scans<sup>16</sup> in the plane containing a\* and b\* through the (1̄,2,0) Bragg peak and the (1̄,2-q<sub>1</sub>,0) satellite peak of an undoped NbSe<sub>3</sub> crystal. The solid line through the Bragg-peak data is the best fit with an assumed Gaussian mosaic distribution. The solid line through the satellite peak is the best fit with the convolution of the Gaussian mosaic distribution and the standard Lorentzian line shape. The HWHM of the Bragg peak is 0.0045° ± 0.0002°. The excess Lorentzian width of the CDW satellite is 0.00094° ± 0.0002°, consistent with the expected amount of dispersive broadening.<sup>17</sup> Assuming that all of the satellite-peak width is due to the CDW correlation length, one obtains an absolute lower bound of l<sub>a\*</sub> ≈ 0.40 μm. If only the excess Lorentzian width is attributed to the CDW correlation length, one obtains l<sub>a\*</sub> ≈ 1.9 μm, a length comparable to the crystal's thickness t = 3.7 μm. This latter estimate does not account for finite-size effects or for dispersive broadening, and thus likely also represents a lower bound for the bulk correlation length.

Figure 2 compares high-resolution scans (using the analyzer crystal) along b\* through the same two peaks.

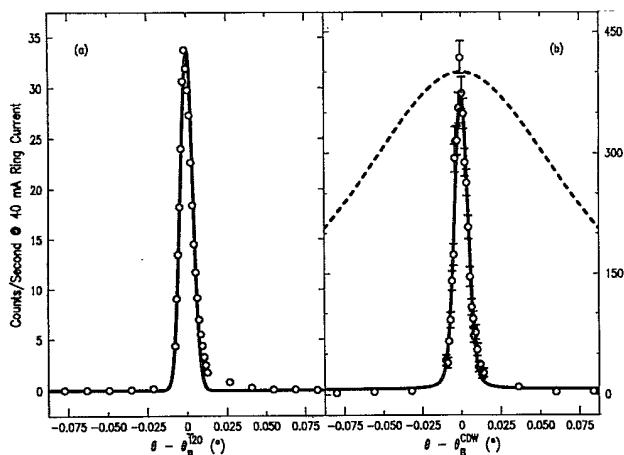


FIG. 1. Mosaic scans in the plane containing a\* and b\* at T ≈ 77 K for an undoped NbSe<sub>3</sub> crystal (r<sub>R</sub> ≈ 300). (a) The (1̄,2,0) Bragg peak. The solid line is the best fit with a Gaussian. The count rates were 1000 times the indicated values. (b) The (1̄,2-q<sub>1</sub>,0) CDW satellite peak. The solid line is the best fit with a Lorentzian convolved with the measured Gaussian mosaic. The dashed line indicates the Lorentzian line shape appropriate for a 200-Å transverse correlation length.

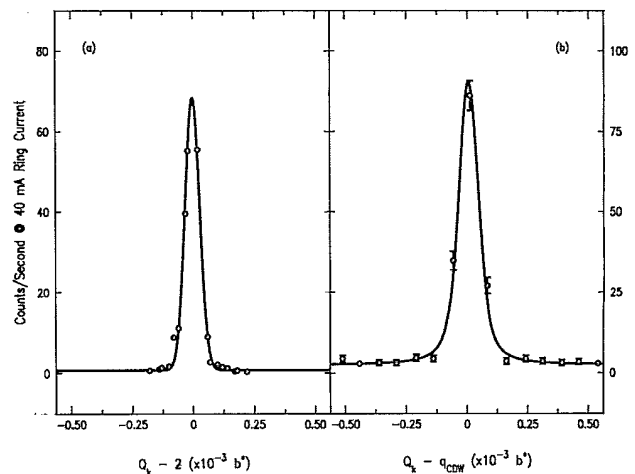


FIG. 2. High-resolution scans along b\* at T ≈ 77 K for the undoped crystal of Fig. 1. (a) The (1̄,2,0) Bragg peak. The solid line is the best fit with a Gaussian resolution. The count rates were 1000 times the indicated values. (b) The (1̄,2-q<sub>1</sub>,0) CDW satellite peak. The solid line is the best fit with a Lorentzian convolved with the measured Gaussian resolution.

The CDW satellite peak is very slightly broadened relative to the Bragg peak. Using the Bragg-peak width of  $(3.5 \pm 0.1) \times 10^{-5} b^*$  as our resolution limit yields an absolute lower bound  $l_{b^*} \approx 1.6 \mu\text{m}$ . Again, one can deconvolve the Gaussian resolution function, yielding an excess Lorentzian width of  $(2.2 \pm 0.4) \times 10^{-5} b^*$  corresponding to  $l_{b^*} \approx 2.5 \mu\text{m}$ . Because of the extremely small peak width and the finite-temperature drift, this length should also be viewed as a lower bound.

Figures 3 and 4 show similar scans for a crystal doped with  $\sim 1800$  ppm Ta per Nb and having  $r_R \approx 10$ . Both the mosaic scan and the high-resolution scan along  $\mathbf{b}^*$  through the CDW satellite peak are significantly broadened relative to the Bragg peak. Further, while both scans through the Bragg peak are well described by Gaussians, Lorentzians are required to fit the CDW scans, indicating fluctuation-dominated broadening. The excess Lorentzian widths are  $0.017^\circ \pm 0.001^\circ$  in the mosaic scan and  $(6.2 \pm 0.7) \times 10^{-5} b^*$  in the  $\mathbf{b}^*$  scan, corresponding to  $l_{a^*} \approx 0.10 \mu\text{m}$  and  $l_{b^*} \approx 0.9 \mu\text{m}$ . The ratio  $l_{b^*}/l_{a^*} \approx 10$  is a factor of 3 larger than the anisotropy of CDW fluctuations above  $T_{P1}$  reported by Moudzen *et al.*<sup>14</sup> In Rb- and W-doped  $\text{K}_{0.3}\text{MoO}_3$ , the measured longitudinal and transverse correlation lengths have comparable magnitudes.<sup>18,19</sup>

We have also studied a crystal containing  $\sim 450$  ppm Ta and having  $r_R \approx 40$ . At this intermediate doping level, the excess Lorentzian widths are  $0.0047^\circ \pm 0.0008^\circ$  and  $(2.8 \pm 0.6) \times 10^{-5} b^*$ , corresponding to  $l_{a^*} \approx 0.37 \mu\text{m}$  and  $l_{b^*} \approx 2.0 \mu\text{m}$ . As in the case of the undoped crystal, this  $l_{b^*}$  value represents a lower bound.

The significant implications of these experimental results are as follows.

(1) Assuming comparable correlation lengths along  $\mathbf{a}^*$  and  $\mathbf{c}$ , a phase-correlated volume in a  $\text{NbSe}_3$  crystal with  $n_i \approx 1800$  ppm Ta contains  $N_i \approx 10^5$  impurities, consistent with weak pinning. The measured ratio of the transverse correlation lengths for the two Ta-doped crystals,  $l_{a^*}(r_R=40)/l_{a^*}(r_R=10) \approx 3.7$ , is consistent with the weak-pinning relation  $l \propto n_i^{-1} \propto r_R$ . Conventional strong-pinning models predict  $N_i \approx 1$  and  $l \approx n_i^{-1/3}$  so that for  $n_i = 1800$  ppm,  $l \approx 50 \text{ \AA}$ . In a revised strong-pinning model,<sup>20</sup>  $l_{a^*} \approx n_i^{-1/3}$  and  $l_{b^*} \propto n_i^{-1}$ . For  $n_i = 1800$  ppm, this model predicts that  $N_i \approx 35$ ,  $l_{a^*} \approx 50 \text{ \AA}$ , and  $l_{b^*} \approx 0.07 \mu\text{m}$ . Strong-pinning models are thus ruled out as viable descriptions of the  $\mathbf{q}_1$  CDW in pure and Ta-doped  $\text{NbSe}_3$ .

(2) From "domains" observed in dark-field TEM images of the CDW superlattice<sup>21</sup> and from analyses of the low-frequency dielectric constant and narrow-band noise, the  $\mathbf{q}_1$  CDW correlation lengths in typical undoped crystals ( $r_R \approx 150$ ) have been estimated (e.g., in Ref. 10) to be  $l_{b^*} \approx 2 \mu\text{m}$  and  $l_{a^*} \approx 200 \text{ \AA}$ . This  $l_{a^*}$  estimate is clearly inconsistent with the measured x-ray peak width, as shown in Fig. 1(b). Extrapolating from our results for  $r_R = 10$  and 40 to  $r_R = 150$  using the weak-pinning relation  $l \propto r_R$  yields correlation lengths  $l_{b^*} \approx 14 \mu\text{m}$  and  $l_{a^*} \approx 1.5 \mu\text{m}$ . These discrepancies indicate that the TEM domains do not reflect CDW phase correlations in bulk  $\text{NbSe}_3$  (Ref. 22) (consistent with subsequent TEM experiments<sup>23</sup>), and that the standard bulk dielectric constant and narrow-band noise analyses are not appropriate.

(3) In undoped  $\text{NbSe}_3$ , the CDW correlation length along  $\mathbf{a}^*$  is comparable to the thickness  $t$  of ordinary crystals. Theoretical and experimental studies of CDWs

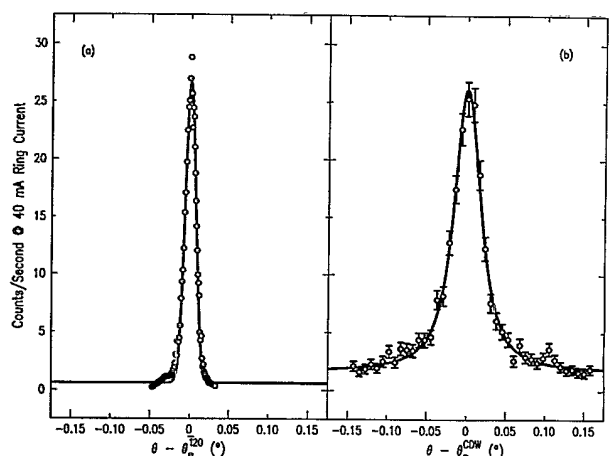


FIG. 3. Mosaic scans in the plane containing  $\mathbf{a}^*$  and  $\mathbf{b}^*$  at  $T \approx 77$  K for a Ta-doped  $\text{NbSe}_3$  crystal having  $r_R \approx 10$ . (a) The  $(\bar{1}, 2, 0)$  Bragg peak. The solid line is the best fit with a Gaussian. The count rates were 1000 times the indicated values. (b) The  $(\bar{1}, 2 - q_1, 0)$  CDW satellite peak. The solid line is the best fit with a Lorentzian convolved with the measured Gaussian mosaic.

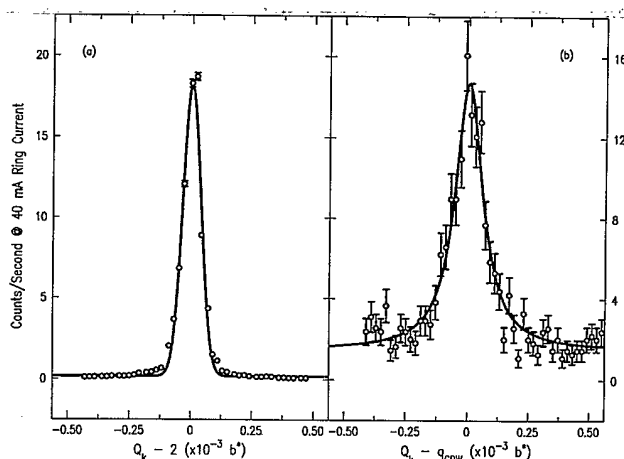


FIG. 4. High-resolution scans along  $\mathbf{b}^*$  at  $T \approx 77$  K for the Ta-doped crystal of Fig. 3. (a) The  $(\bar{1}, 2, 0)$  Bragg peak. The solid line is the best fit with a Gaussian resolution function. The count rates were 1000 times the indicated values. (b) The  $(\bar{1}, 2 - q_1, 0)$  CDW satellite peak. The solid line is the best fit with a Lorentzian convolved with the measured Gaussian resolution.

in this material thus must explicitly account for sample dimensions.

(4) The result  $l_a^* \sim t$  provides strong additional evidence for McCarten *et al.*'s weak-pinning dimensionality-crossover interpretation of the size dependence of  $E_T$ . From the crystal thickness at which the crossover from bulk (3D) to size-dependent (2D) behavior of  $E_T$  is observed, the correlation length was estimated in Ref. 6 as  $l_a^* \approx 0.019r_R \mu\text{m}$ , in factor-of-2 agreement with the lengths measured here.

In conclusion, we have determined the length scales for CDW phase correlations in NbSe<sub>3</sub>. Together with the results of earlier transport measurements, these lengths establish the essential character of CDW pinning in pure and Ta-doped NbSe<sub>3</sub>: It is weak, and exhibits a dimensionality crossover as a function of crystal thickness. System size and pinning dimensionality must therefore be important parameters in future work on CDW pinning and dynamics.

We wish to thank B. Batterman, John Bardeen, R. M. Fleming, J. C. Gill, J. McCarten, and F. Levy for fruitful discussions. J.D.B. acknowledges support provided by Cornell's Materials Science Center (NSF Grant No. DMR88-18558-A02). R.E.T. acknowledges support provided by the Alfred P. Sloan Foundation, by the AT&T Foundation, and by the NSF (Grant No. DMR-8958515). CHESS is supported by the NSF (Grant No. DMR87-19764).

<sup>1</sup>H. Fukuyama and P. A. Lee, Phys. Rev. B **17**, 535 (1978); P. A. Lee and T. M. Rice, Phys. Rev. B **19**, 3970 (1979).

<sup>2</sup>S. Abe, J. Phys. Soc. Jpn. **54**, 3494 (1985); **55**, 1987 (1986).

<sup>3</sup>J. W. Brill, N. P. Ong, J. C. Eckert, J. W. Savage, S. K. Khanna, and R. B. Somoano, Phys. Rev. B **23**, 1517 (1981).

<sup>4</sup>M. Underweiser, M. Maki, B. Alavi, and G. Grüner, Solid State Commun. **64**, 181 (1987).

<sup>5</sup>P. Monceau, Physica (Amsterdam) **109B**, 1890 (1982).

<sup>6</sup>J. McCarten, M. Maher, T. L. Adelman, and R. E. Thorne, Phys. Rev. Lett. **63**, 2841 (1989).

<sup>7</sup>D. V. Borodin, F. Ya. Nad', S. Savitskaja, and S. V. Zaitsev-Zotov, Physica (Amsterdam) **143B**, 73 (1986).

<sup>8</sup>P. J. Yetman and J. C. Gill, Solid State Commun. **62**, 201

(1987).

<sup>9</sup>For a detailed discussion of the weak-pinning theory of size effects, see John Bardeen, Phys. Rev. Lett. **64**, 2297 (1990).

<sup>10</sup>J. R. Tucker, Phys. Rev. Lett. **65**, 270 (1990); J. C. Gill, *ibid.* **65**, 271 (1990).

<sup>11</sup>R. E. Thorne and J. McCarten, Phys. Rev. Lett. **65**, 272 (1990).

<sup>12</sup>J. L. Hodeau, M. Marezio, C. Roucau, R. Ayroles, A. Meerschaut, J. Rouxel, and P. Monceau, J. Phys. C **11**, 4117 (1978).

<sup>13</sup>R. M. Fleming, D. E. Moncton, J. D. Axe, and G. S. Brown, Phys. Rev. B **30**, 1877 (1984).

<sup>14</sup>A. H. Moudden, J. D. Axe, P. Monceau, and F. Levy, Phys. Rev. Lett. **65**, 223 (1990).

<sup>15</sup>Finite-size effects produce large crystal-to-crystal variations in  $E_T$  (Refs. 6-8) and  $r_R$  (Ref. 6). The quoted  $E_T$  and  $r_R$  values are thus averages for large crystals, representing the bulk values characteristic of the growths from which the crystals studied here were taken.

<sup>16</sup>The  $\theta$  rocking curves were taken without the analyzer crystal.

<sup>17</sup>The uncertainties in the line widths correspond to a doubling of  $\chi^2$ .

<sup>18</sup>T. Tamegai, K. Tsutsumi, and S. Kagoshima, Synth. Met. **19**, 923 (1987).

<sup>19</sup>For an excellent review of x-ray studies of K<sub>0.3</sub>MoO<sub>3</sub>, see J. P. Pouget, in *Low-Dimensional Electronic Properties of Molybdenum Bronzes and Oxides*, edited by C. Schlenker (Kluwer, Dordrecht, 1989), p. 87.

<sup>20</sup>J. R. Tucker, W. G. Lyons, and G. Gammie, Phys. Rev. B **38**, 1148 (1988); **40**, 5447 (1989).

<sup>21</sup>K. K. Fung and J. W. Steeds, Phys. Rev. Lett. **45**, 1696 (1980). Interpretation of TEM images of the CDW in terms of pinning-related phase correlations was suggested but not accepted by these authors. [See C. H. Chen, R. M. Fleming, and P. M. Petroff, Phys. Rev. B **27**, 4459 (1983); J. W. Steeds, K. K. Fung, and S. McKernan, J. Phys. C **3**, 1623 (1983).]

<sup>22</sup>In 2D weak pinning,  $l_a^* \approx t$  and  $l_b^*$  and  $l_c^*$  are proportional to  $\sqrt{t}$  (Ref. 11). Using  $t = 500 \text{ \AA}$ , typical of the TEM samples, and assuming that  $r_R = 150$  and that  $l_c^*/l_b^*$  has the same ratio as found in Ref. 14 for CDW fluctuations above  $T_{P1}$ , we estimate  $l_b^* \approx 2.6 \mu\text{m}$  and  $l_c^* \approx 100 \text{ \AA}$ , close to the TEM domain dimensions. However, the significance of this agreement and the origin of the TEM domains is unclear (Ref. 11).

<sup>23</sup>Chen, Fleming, and Petroff (Ref. 20); Steeds, Fung, and McKernan (Ref. 20).